Lithuanian Journal of Physics, Vol. **58**, No. 3, pp. 267–276 (2018)

COMPARISON BETWEEN MAGNETIC PROPERTIES OF $CoFe_2O_4$ AND $CoFe_2O_4$/POLYPYRROLE NANOPARTICLES

K. Mažeika [a], V. Bėčytė [a], Yu.O. Tykhonenko-Polishchuk [b], M.M. Kulyk [c], O.V. Yelenich [d], and A.I. Tovstolytkin [b]

[a] *State Research Institute Center for Physical Sciences and Technology, Savanorių 231, 02300 Vilnius, Lithuania*
[b] *Institute of Magnetism of the NAS of Ukraine and MES of Ukraine, 36-b Vernadsky Blvd., 03142 Kyiv, Ukraine*
[c] *Institute of Physics of the NAS of Ukraine, 46 Nauky Ave., 03028 Kyiv, Ukraine*
[d] *V.I. Vernadskii Institute of General and Inorganic Chemistry of the NAS of Ukraine, 32/34 Palladina Ave., 03142 Kyiv, Ukraine*
Email: kestutis.mazeika@ftmc.lt

Received 27 April 2018; revised 28 June 2018; accepted 15 October 2018

$CoFe_2O_4$/polypyrrole composite nanoparticles were synthesized using a high energy ball mill. Mössbauer and Fourier transform infrared spectroscopies, magnetization measurements and transmission electron microscopy were used for the characterization of samples. Specific loss power (*SLP*) was determined by exposing nanoparticles to an alternating magnetic field. Some changes in coercivity were observed and explained comparing $CoFe_2O_4$ nanoparticles with $CoFe_2O_4$/polypyrrole composite nanoparticles.

Keywords: nanocomposites, magnetic materials, hyperthermia, ferrite

PACS: 62.23.Pq, 75.50.Tt, 76.80.+y

1. Introduction

Composites of organic polymers and iron oxide (γ–Fe_2O_3 and α–Fe_2O_3) or ferrite (Fe_3O_4, $CoFe_2O_4$ and $MnFeO_4$) nanoparticles were studied as prospective sorbents as well as materials for electrocatalytic and biomedical applications [1–7]. Polypyrrole (PPy) stands out as a widely used conducting polymer suitable for gas sensor, biosensor and biomedical applications because of good physical properties as well as an easy synthesis [1, 2, 8, 9]. Ferrite Fe_3O_4 and $CoFe_2O_4$ nanoparticles are chemically stable and have good magnetic properties. The potential of application of magnetic nanoparticles (MNPs) in biomedicine for cell separation, drug delivery, MRI, hyperthermia, etc. was shown [10–19]. Scientists are trying to find novel ways of the MNPs functionalization considering a long list of requirements, such as controllability of particle size, biocompatibility, chemical stability, thermal response to an alternating magnetic field, etc. Various organic polymers, such as dextran, chitosan, polyethylene glycol (PEG) and others [4, 16, 20], have been used as coating materials.

For more than half a century mainly magnetite Fe_3O_4 nanoparticles have been applied for *in vitro* studies. However, cobalt ferrite $CoFe_2O_4$ MNPs can also be an attractive candidate for hyperthermia treatment due to high anisotropy and magnetisation as well as good chemical stability [21]. Because of high anisotropy, a smaller size of $CoFe_2O_4$ nanoparticles may be used if applying hysteresis losses as a source of heating for hyperthermia treatment [22]. Moreover, according to Pašukonienė et al. [23] superparamagnetic cobalt

ferrite nanoparticles synthesized by co-precipitation are non-toxic to human pancreatic and ovarian cancer cells at low concentrations. It was also found that the antibacterial effect against *E. coli* and *S. aureus* increased when zinc and copper partially substituted cobalt in $CoFe_2O_4$ nanoparticles [24]. Moreover, it was found that antimicrobial properties of cobalt ferrite nanoparticles depend on the size of nanoparticles [25].

It is well known that physical and chemical properties of nanoparticles depend on the synthesis method. Among many different methods to synthesize nanoparticles, the mechanochemical method has been recently shown to be an effective way to produce large quantities of nanoparticles [26]. High energy milling in a steel vial containing 1 200 steel balls also provide a possibility of intense mixing preventing the formation of large $CoFe_2O_4$/PPy composite nanoparticles. The previous studies [4, 6, 7] showed that adding of organic polymers in the composites with $CoFe_2O_4$ nanoparticles influenced the magnetic properties (coercivity and remanence). Therefore, the aim of the study was to synthesize $CoFe_2O_4$/PPy composite nanoparticles which can be dispersible in liquids, controlled by magnetic field, and suitable for biomedical applications, and to investigate the influence of polypyrrole on magnetic and hyperthermia treatment related properties. We studied magnetic as well as high-frequency magnetic field heating characteristics of $CoFe_2O_4$ nanoparticles, separately and in the $CoFe_2O_4$/PPy composite. Magnetic properties were compared at different temperature.

2. Experiment

2.1. Materials and methods

Magnetic cobalt ferrite nanoparticles (8–10 nm in diameter) have been synthesized according to Ref. [26]. One hundred millilitres of cobalt ferrite nanofluid stabilized with citric acid was mixed with a 2 ml pyrrole monomer for 1 minute at a rotational speed of 400 rpm in a Fritch Pulverisette 6 (*Fritsch GmbH*) mill steel vial containing 1 200 steel balls, each 5 mm in diameter. Four grams of $FeCl_3 \cdot 6H_2O$ were added as a polymerization initiator. The prepared samples of composite nanoparticles were centrifuged and washed with deionized water for several times.

2.2. Characterization techniques

Mössbauer spectra were collected in the transmission geometry using a ^{57}Co(Rh) source. Mössbauer spectra were fitted applying the WinNormos (Site, Dist) software. The images of synthesized composite nanoparticles were obtained using a transmission electron microscope Tecnai G2 F20 X-TWIN (*FEI*, Netherlands, 2011). Fourier transform infrared spectroscopy spectra were obtained using a Vertex 70v spectrometer. Magnetic measurements were performed in the ±10 kOe magnetic field at temperatures of 100–340 K using an LDJ-9500 vibrating sample magnetometer. For the calorimetric determination of specific loss power (*SLP*), which is released on the exposure of an ensemble of the particles to the applied alternating magnetic field (AMF), ferrofluids based on the synthesized MNPs were prepared using 0.1% aqueous agarose solutions [27]. The concentration of MNP ferrofluids was about 5 mg/ml. The prepared ferrofluids were placed in the middle of a magnetic coil (5 turns, 3 cm diameter) which induced AMF with a frequency of 300 kHz and amplitudes up to 124 Oe (9.9 kA/m). All calorimetric measurements have been carried out according to the procedure described by Veverka et al. [28]. *SLP* values were calculated according to

$$SLP = \frac{C_{\text{fluid}} \cdot V_{\text{s}}}{m_{\text{powder}}} \cdot \frac{\mathrm{d}T_{\text{fluid}}}{\mathrm{d}\tau}, \qquad (1)$$

where $\mathrm{d}T_{\text{fluid}}/\mathrm{d}\tau$ is the initial slope of the graph of change in temperature versus time, C_{fluid} and V_{s} are the volumetric specific heat and volume of the solution, respectively, and m_{powder} is the mass of magnetic material in the fluid.

3. Results and discussion

3.1. Mössbauer data and structural properties

Mössbauer spectra of $CoFe_2O_4$ nanoparticles and $CoFe_2O_4$/PPy composite nanoparticles collected at room temperature are shown in Fig. 1. For both measured samples, the spectra consist of a doublet and a sextet shaped pattern typical of nanostructural ferrite. Both magnetically split (sextet) and non-magnetic (doublet) subspectra appear because of the nanoparticle size distribution in

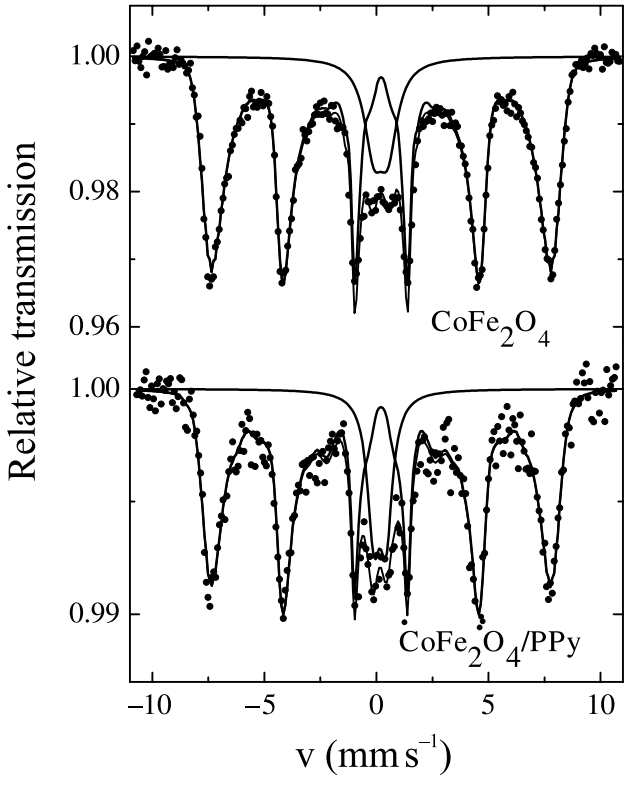

Fig. 1. Mössbauer spectra of pure $CoFe_2O_4$ and polypyrrole coated cobalt ferrite $CoFe_2O_4$/PPy.

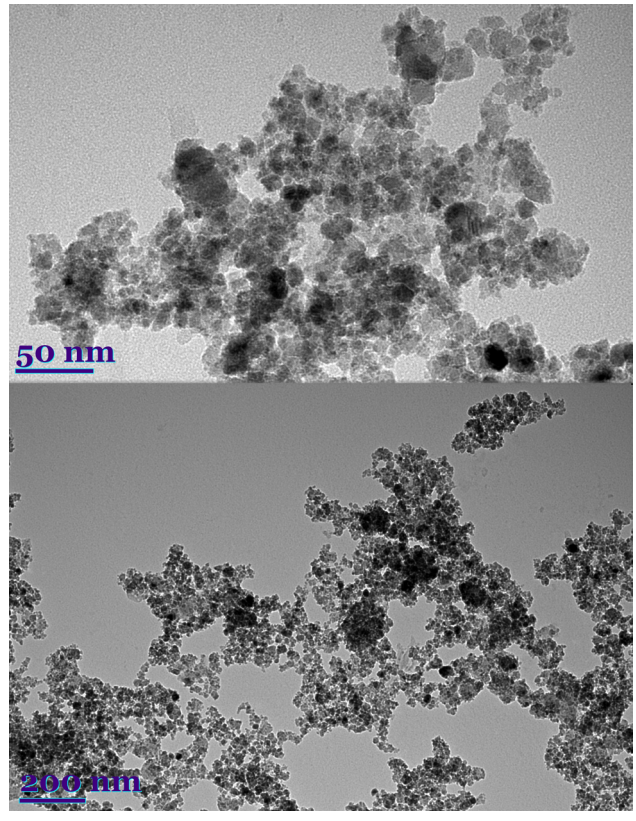

Fig. 2. TEM image of polypyrrole coated cobalt ferrite nanoparticles.

the samples [26]. A small area of the doublet (15 and 13%, respectively, for $CoFe_2O_4$ and $CoFe_2O_4$/PPy) suggests that for the majority of MNPs causing a magnetically split component of the spectra the magnetic moment is in a blocked state at room temperature [29]. The broadened lines of the sextet pattern characterized by the average hyperfine field of 40 T which is 20% lower than that of bulk $CoFe_2O$ [30] indicate collective excitations of magnetic moments of nanoparticles. Figure 2shows the TEM images of $CoFe_2O_4$/polypyrrole. As reported earlier [26], the size D of synthesized pure cobalt ferrite MNPs was estimated to be 8–10 nm. Figure 3 shows the FTIR spectra of the pure polypyrrole and $CoFe_2O_4$/PPy composite. The characteristic absorption peak of $CoFe_2O_4$ at 574 cm^{-1}, which arises due to the stretching vibration of Fe(Co)–O, is clearly seen in the spectrum. All the characteristic absorption peaks of polypyrrole arising due to the N–H stretching, C–C out-of-plane deformation, backbone C=C stretching, and C–H out-of-plane deformation vibrations are clearly visible in the $CoFe_2O_4$/PPy spectrum which is almost identical to that of pure polypyrrole [31].

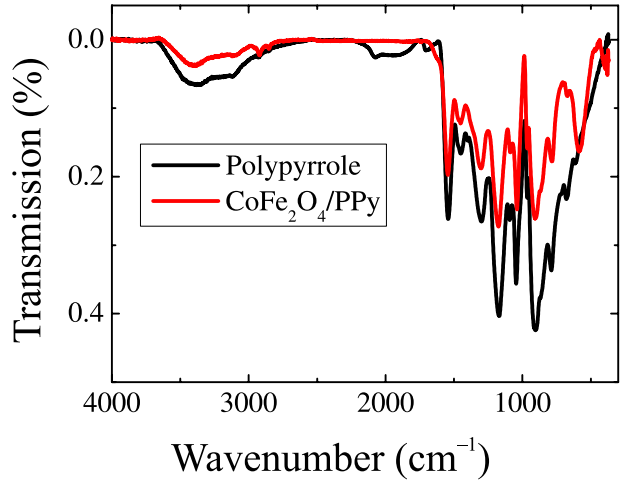

Fig. 3. FT-IR spectra of polypyrrole and polypyrrole coated MNPs.

3.2. Magnetic properties

Figure 4 shows the magnetization curves $M(H)$ for pure $CoFe_2O_4$ and $CoFe_2O_4$/PPy MNPs measured at temperatures T = 100 K (Fig. 4(a)) and T = 288 K (Fig. 4(b)). MNPs of both compositions exhibit a strong hysteresis and have a relatively large magnetization both at low and high temperatures. In

high magnetic fields magnetization has the pronounced tendency towards saturation. The saturation magnetization values (defined as magnetization in 10 kOe field), $M_s^{CoFe_2O_4}$ = 28 emu/g and $M_s^{CoFe_2O_4/PPy}$ = 20 emu/g, have been estimated at low temperature (100 K). At room temperature (288 K) the values of saturation magnetization $M_s^{CoFe_2O_4}$ = 25 emu/g and $M_s^{CoFe_2O_4/PPy}$ = 19.5 emu/g have been obtained.

The saturation magnetization value for the bulk $CoFe_2O_4$ is $M_s \approx 94$ emu/g [32]. In comparison with the bulk saturation magnetization the obtained experimental values of M_s are ~4 times smaller. This is likely to result from a noticeable contribution of the subsurface layers of MNPs which, as a rule, are partly or completely magnetically disordered [33]. For all the MNPs under consideration, the curves of magnetization M versus the magnetic field H have hysteresis at both temperatures.

The coercivity values $H_c^{CoFe_2O_4}$ = 3280 Oe and $H_c^{CoFe_2O_4/PPy}$ = 2720 Oe at 100 K have been estimated (see the inset in Fig. 4(a)). At room temperature, coercivity values are almost by one order of magnitude smaller: $H_c^{CoFe_2O_4}$ = 370 Oe and $H_c^{CoFe_2O_4/PPy}$ = 300 Oe, respectively (see the inset in Fig. 4(b)). A peculiar feature for the sample coated with PPy is a steep inflection of the magnetization curve in the vicinity of zero field, which is observed at low temperature (see Fig. 4(a); marked by a dashed line). This means that the MNPs of this composition can easily rotate under an external magnetic field. On the other hand, the MNPs without PPy coating are strongly pinned and do not move, which explains the absence of such inflection in their hysteresis loop $M(H)$ at 100 K (it should be noted that both powders were densely packed in a plastic container). However, the inflection disappeared in a hysteresis loop of additionally glued $CoFe_2O_4$/PPy (Fig. 4(c)) suggesting that the observed inflection is due to the rotation of PPy glued agglomerates of $CoFe_2O_4$ nanoparticles. Possibly, because of high magnetic anisotropy at low temperature, $CoFe_2O_4$/PPy composite particles can rotate if the particle sticking is not very good. It is noteworthy that nanoparticle agglomerates are nonuniform, of different size and shape, as observed in the TEM images (Fig. 2). Moreover, the enhanced mobility in magnetic field and lower ferrofluid stability compared with the case of $CoFe_2O_4$ MNPs can be associated with forming of large $CoFe_2O_4$/PPy composite particles which interact more strongly between themselves and with magnetic field.

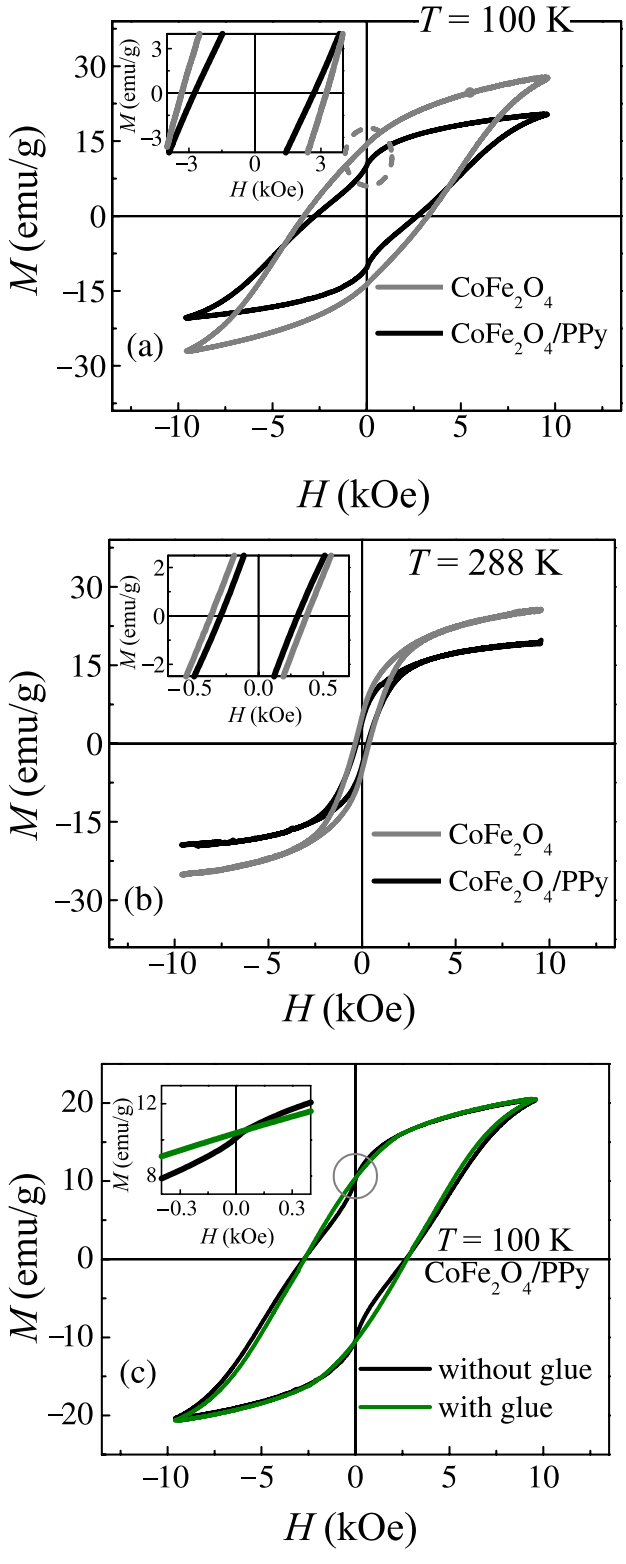

Fig. 4. Hysteresis loops $M(H)$ for pure $CoFe_2O_4$ and $CoFe_2O_4$/PPy MNPs measured at 100 (a), 288 (b) and at 100 K glued and free $CoFe_2O_4$/PPy (c). The inset shows the same dependences in the region of low fields.

Temperature dependences of magnetization (Fig. 5) were obtained in two different measurement modes: zero-field-cooling (ZFC) and field-cooling (FC). In the ZFC mode, a sample was cooled down to 100 K in the zero magnetic field. At this temperature, the external magnetic field H_{measur} was applied to the sample and M_{ZFC} was measured as a function of T in the process of sample heating. In the FC mode, the sample was cooled in the magnetic field $H_{cooling} = H_{measur}$. For the MNPs under study measurements were carried out in the applied magnetic field H_{measur} = 187 Oe. The obtained magnetization dependences on the temperature $M_{ZFC}(T)$ and $M_{FC}(T)$ for the samples of both pure $CoFe_2O_4$ and $CoFe_2O_4$/PPy are shown in Fig. 5(a, b), respectively.

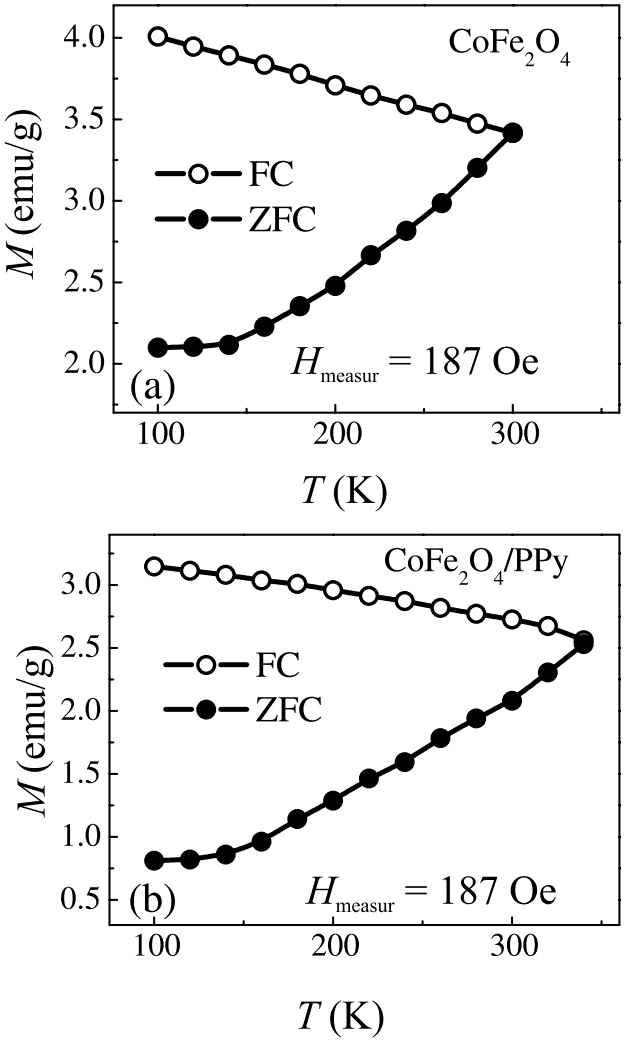

Fig. 5. Temperature dependences of magnetization M (ZFC- and FC-measurements) for pure $CoFe_2O_4$ (a) and $CoFe_2O_4$/PPy (b) MNPs. Measurements were carried out in magnetic field H_{measur} = 187 Oe.

An important parameter that characterizes the behaviour of MNPs is the blocking temperature T_b, at which the magnetization M_{ZFC} measured in a weak magnetic field achieves the maximum. Above the blocking temperature, the magnetic state of single domain MNPs is characterized as superparamagnetic (when the ensemble of particles behaves like a paramagnet consisting of MNPs with very large magnetic moments [34, 35]) and the system does not show any hysteresis. Below T_b, the MNPs are in a blocked state (particle moments appear frozen on the time of measurement [34]) and their behaviour is characterized by hysteresis. In our case, for both samples, M_{ZFC} displays growth below and above room temperature. This means that the blocking temperature for both samples exceeds room temperature, and thus at 288 K they are in a blocked state. This is also confirmed by the presence of hysteresis with ~300 Oe coercivity and a very strong tendency of magnetization towards saturation at room temperature.

It is hard to define the exact mass ratio of PPy and $CoFe_2O_4$ in the synthesized composite. The $CoFe_2O_4$ nanoparticles are covered by a surfactant (citric acid) and only part of all PPy can be bound to $CoFe_2O_4$ nanoparticles. Polypyrrole in samples can explain the observed 22–29% decrease in saturation magnetization. The coercivity H_c decreases as a result of adding PPy by 17 and 19%, at 100 K and room temperature, respectively. The relative remanence $r_m = M(H = 0)/M_s$ is approximately the same (≈0.5 at 100 K and ≈0.2 at 288 K temperature) for the $CoFe_2O_4$ and $CoFe_2O_4$/PPy samples. The effects of polymers on H_C and r_m were previously found to differ for various composites of $CoFe_2O_4$ nanoparticles with the organic polymers – polypyrrole (PPy), poly(aniline) (PANI) and polyethylenedioxythiophene (PEDOT) [6, 7]. For $CoFe_2O_4$/PPy composites H_c decreases when the amount of PPy increases but r_m does not change [6]. For $CoFe_2O_4$/PANI and $CoFe_2O_4$/PEDOT composites r_m increases with the polymer amount while H_c decreases first and later increases when adding PANI and PEDOT polymers [6, 7]. Values of the relative remanence were found to be in a range of 0.2–0.3 [6, 7].

For the non-interacting nanoparticles of volume V and magnetic uniaxial anisotropy K the coercivity is given by

$$H_c = H_K\left(1-\left(\frac{\ln(\tau_m/\tau_0)kT}{KV}\right)^{2/3}\right) = H_K\left(1-\left(\frac{T}{T_b}\right)^{2/3}\right), \quad (2)$$

where $H_K = 2K/M_s$ is the anisotropy field, k is the Boltzmann constant, T is temperature, τ_m is the characteristic measurement time and τ_0 is the inverse superparamagnetic attempt frequency [36]. The blocking temperature is $T_b = KV/k\ \ln(\tau_m/\tau_0)$. For $CoFe_2O_4$ nanoparticles H_c may reach some kOe at low temperature [37], but the highest switching field for $CoFe_2O_4$ given by H_K is not achieved.

The influence of magnetic interactions was shown for the $CoFe_2O_4$ nanoparticles in composites with polymers and Au [6, 7, 29]. The indirect exchange coupling of RKKY (Ruderman–Kittel–Kasuya–Yosida) through conducting electrons was used to explain the changes in magnetization loops of $CoFe_2O_4$ nanoparticles mixed with conductive polyaniline [7]. Polypyrrole is also known to have good conductive properties [9]. When the interactions between nanoparticles couple the magnetic moments antiferromagnetically, H_c decreases [36]. The relative remanence of ≈0.2 of our samples indicates that the influence of inter-particle interactions dominates [35]. Applying the random anisotropy model for soft magnetic nanocrystalline materials the effective anisotropy is defined as $K_{eff} = K/\sqrt{N}$, where N is the number of correlated nanoparticles [38, 39]. As the correlation length $L_{ex} = \sqrt{A/K_{eff}}$, where A is the exchange stiffness, the effective anisotropy

$$K_{eff} = K^4D^6/A^3. \quad (3)$$

The random anisotropy model was found to be applicable even when dipolar interactions were dominating [39].

The role of inter-particle interactions relative to the anisotropy energy decreases with temperature decrease as the relative remanence r_m increases [35]. In Refs. [6, 7] the changes in H_c and r_m were explained by the polymer induced modifications of surface anisotropy and magnetic interactions. The superparamagnetic relaxation of nanoparticles and the decrease in effective anisotropy K_{eff} according to Eq. (2) would cause reduction in H_c when temperature increases. It is noteworthy that Eq. (3) indicates the sensitivity of the effective anisotropy K_{eff} to any changes in the magnetic anisotropy K and the exchange stiffness A either due to temperature variation or polymer coating.

3.3. Heating characteristics for hyperthermia application

To obtain AC magnetic heating characteristics for the synthesized MNPs, magnetic fluids of $CoFe_2O_4$ and $CoFe_2O_4$/PPy MNPs have been prepared. Changes in the temperature (T_{fluid}) of the fluids in dependence on the residence time τ have been studied. Figure 6 shows the dependences $T_{fluid}(\tau)$ obtained for both compositions. The measurements were carried out in an external AMF with the fixed frequency f of 300 kHz and the amplitude H_{max} of 124 Oe (9.9 kA/m). The initial slope of each curve $dT_{fluid}/d\tau$ plotted in Fig. 6 provides information about *SLP*. Using Eq. (1), the following experimental values of *SLP* were obtained for the ensembles of cobalt ferrite MNPs: $SLP^{CoFe_2O_4}$ = 15.4 W/g and $SLP^{CoFe_2O_4/PPy}$ = 11.3 W/g.

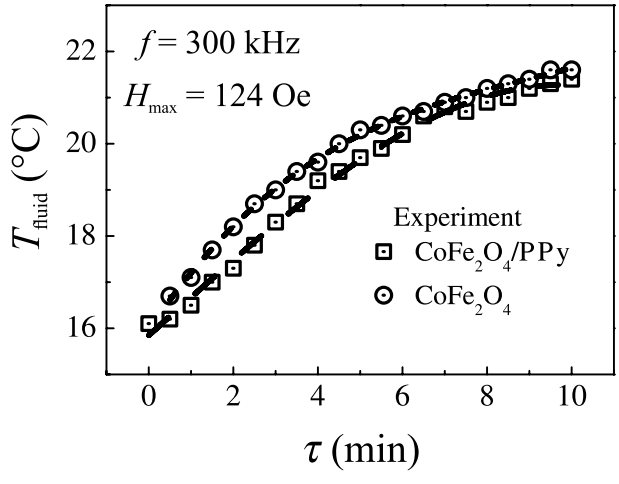

Fig. 6. Time dependences of heat generation for the ferrofluids based on synthesized MNPs of pure $CoFe_2O_4$ and $CoFe_2O_4$/PPy. The measurements were carried out in AMF with the fixed frequency f = 300 kHz and amplitude H_{max} = 124 Oe (9.9 kA/m). The values obtained by the experiment are marked as symbols (circles and squares) while dashed lines show the results of fitting by the polynomial function $T_{fluid} = a + b\tau + c\tau^2 + d\tau^3$ denoted as dashed lines.

In order to theoretically study the heating characteristics of the synthesized MNPs in the external field (f = 300 kHz and H_{max} = 124 Oe), the features of the magnetic state at 288 K have been taken into account for both compositions. Since MNPs of both pure $CoFe_2O_4$ and $CoFe_2O_4$/PPy samples are characterized by a blocked state (see Fig. 5) and the presence of hysteresis at 288 K (see Fig. 4), the Stoner–Wohlfarth model was used for estimation of the maximally possible value of *SLP* [34, 40]. In this case for the ensemble of MNPs placed in the external AMF the magnitude of heat dissipated by MNPs during one magnetization cycle equals the hysteresis loop area *S*.

If the magnetization is normalized per unit of MNPs mass, the *SLP* magnitude is defined as

$$SLP_{SW} = S \cdot f. \quad (4)$$

In the general case for the ensemble of MNPs with randomly oriented anisotropy axes the upper limit value of SLP is [34]

$$SLP_{SW}^{limit} = 4\alpha\mu H_{max} M_s f, \quad (5)$$

where α = 0.39 [40, 41] is a dimensionless parameter which equals the ratio between the areas of the actual hysteresis loop and the ideal rectangle loop, with the latter having α = 1, and M_s is the saturation magnetization of MNPs. Thus for $CoFe_2O_4$ and $CoFe_2O_4$/PPy compositions the upper limits of *SLP*, calculated according to Eq. (5), are $SLP^{(limit)CoFe_2O_4}$= 145.1 W/g and $SLP^{(limit)CoFe_2O_4/PPy}$ = 113.2 W/g. It should be noted that Eq. (5) is valid only in the case when the amplitude of AMF exceeds the coercivity. In our case this condition is not met (H_{max} = 124 Oe while coercivities are $H_c^{CoFe_2O_4}$ = 370 Oe and $H_c^{CoFe_2O_4/PPy}$ = 300 Oe, respectively (see Fig. 4)). However, Eq. (5) shows the maximally possible value of *SLP* that may potentially be achieved in cobalt spinel MNPs.

4. Conclusions

This work demonstrates promising prospects of the fabrication of $CoFe_2O_4$/polypyrrole composite nanoparticles dispersed in ferrofluid by high energy milling and shows the directions for tuning their properties to meet the requirements necessary for development of biomedical applications. The FT-IR spectra and TEM images indicate that $CoFe_2O_4$/polypyrrole composite nanoparticles were successfully prepared as pollypyrole glued $CoFe_2O_4$ nanoparticles. The magnetic properties and heating characteristics for hyperthermia treatment somewhat differ between the $CoFe_2O_4$ and $CoFe_2O_4$/polypyrrole composite nanoparticles. The coercivity decreases when forming a nanocomposite with polypyrrole at 100 and 288 K by 17–19% indicating that the effect of polypyrrole is weakly temperature dependent. The change in coercivity can be explained in terms of the effective anisotropy of strongly interacting nanoparticles influenced by coating with polypyrrole.

Acknowledgements

The work is partially supported by the Ministry of Science and Education of Ukraine through the Project 'Micro- and Nanofluidics in Stray Magnetic Fields of Artificial and Biogenic Magnetic Particles' (Reg. No. 0118U003790). We are grateful to M. Kirsnytė for the FT-IR spectra and to M. Skapas for the TEM images.

References

[1] F.A. Harraz, A.A. Ismail, A.A. Al-Sayari, and A. Al-Hajry, Novel α-Fe_2O_3/polypyrrole nanocomposite with enhanced photocatalytic performance, J. Photochem. Photobiol. A **299**, 18–24 (2015), https://doi.org/10.1016/j.jphotochem.2014.11.001

[2] M.V. Murugendrappa and M.V.N. Ambika Prasad, Dielectric spectroscopy of polypyrrole–γ–Fe_2O_3 composites, Mater. Res. Bull. **41**, 1364–1369 (2006), https://doi.org/10.1016/j.materresbull.2005.12.011

[3] H. Zhao, M. Huang, J. Wu, L. Wang, and H. He, Preparation of Fe_3O_4@PPy magnetic nanoparticles as solid-phase extraction sorbents for preconcentration and separation of phthalic acid esters in water by gas chromatography–mass spectrometry, J. Chromatogr. B **1011**, 33–44 (2016), https://doi.org/10.1016/j.jchromb.2015.12.041

[4] C.I. Covaliu, I. Jitaru, G. Paraschiv, E. Vasile, S.S. Biriş, L. Diamandescu, V. Ionita, and H. Iovu, Core–shell hybrid nanomaterials based on $CoFe_2O_4$ particles coated with PVP or PEG

biopolymers for applications in biomedicine, Powder Technol. **237**, 415–426 (2013), https://doi.org/10.1016/j.powtec.2012.12.037

[5] R.N. Singh, B. Lal, and M. Malviya, Electrocatalytic activity of electrodeposited composite films of polypyrrole and $CoFe_2O_4$ nanoparticles towards oxygen reduction reaction, Electrochim. Acta **49**, 4605–4612 (2004), https://doi.org/10.1016/j.electacta.2004.05.015

[6] I.M. Resta, G. Horwitz, M.L.M. Elizalde, G.A. Jorge, F.V. Molina, and P.S. Antonel, Magnetic and conducting properties of composites of conducting polymers and ferrite nanoparticles, IEEE T. Magn. **49**, 4598–4601 (2013), https://doi.org/10.1109/TMAG.2013.2259582

[7] P.S. Antonel, F.M. Berhó, G. Jorge, and F.V. Molina, Magnetic composites of $CoFe_2O_4$ nanoparticles in a poly(aniline) matrix: enhancement of remanence ratio and coercivity, Synth. Met. **199**, 292–302 (2015), https://doi.org/10.1016/j.synthmet.2014.12.003

[8] S. Geetha, C.R.K. Rao, M. Vijayan, and D.C. Trivedi, Biosensing and drug delivery by polypyrrole, Anal. Chim. Acta **568**, 119–125 (2006), https://doi.org/10.1016/j.aca.2005.10.011

[9] J.M. Fonner, L. Forciniti, H. Nguyen, J. Byrne, Y.F. Kou, J. Syeda-Nawaz, and C.E. Schmidt, Biocompatibility implications of polypyrrole synthesis techniques, Biomed. Mater. **3**, 034124 (2008), https://doi.org/10.1088/1748-6041/3/3/034124

[10] B.D. Plouffe, S.K. Murthy, and L.H. Lewis, Fundamentals and application of magnetic particles in cell isolation and enrichment: a review, Rep. Prog. Phys. **78**, 016601 (2015), https://doi.org/10.1088/0034-4885/78/1/016601

[11] R. Hergt, S. Dutz, R. Müller, and M. Zeisberger, Magnetic particle hyperthermia: nanoparticle magnetism and materials development for cancer therapy, J. Phys. Condens. Matter **18**, S2919–S2934 (2006), https://doi.org/10.1088/0953-8984/18/38/S26

[12] M. Liong, J. Lu, M. Kovochich, T. Xia, S.G. Ruehm, A.E. Nel, F. Tamanoi, and J.I. Zink, Multifunctional inorganic nanoparticles for imaging, targeting, and drug delivery, ACS Nano **2**(5), 889–896 (2008), https://doi.org/10.1021/nn800072t

[13] D.-H. Kim, D.E. Nikles, D.T. Johnson, and C.S. Brazel, Heat generation of aqueously dispersed $CoFe_2O_4$ nanoparticles as heating agents for magnetically activated drug delivery and hyperthermia, J. Magn. Magn. Mater **320**, 2390–2396 (2008), https://doi.org/10.1016/j.jmmm.2008.05.023

[14] F. Yu, L. Zhang, Y. Huang, K. Sun, A.E. David, and V.C. Yang, The magnetophoretic mobility and superparamagnetism of core-shell iron oxide nanoparticles with dual targeting and imaging functionality, Biomaterials **31**, 5842–5848 (2010), https://doi.org/10.1016/j.biomaterials.2010.03.072

[15] N. Kohler, C. Sun, J. Wang, and M. Zhang, Methotrexate-modified superparamagnetic nanoparticles and their intercellular uptake into human cancer cells, Langmuir **21**, 8858–8864 (2005), https://doi.org/10.1021/la0503451

[16] H. Lee, E. Lee, D.K. Kim, N.K. Jang, Y.Y. Jeong, and S. Jon, Antibiofouling polymer-coated superparamagnetic iron oxide nanoparticles as potential magnetic resonance contrast agents for *in vivo* cancer imaging, J. Am. Chem. Soc. **128**, 7383–7389 (2006), https://doi.org/10.1021/ja061529k

[17] E.Q. Song, J. Hu, C.Y. Wen, Z.Q. Tian, X. Yu, Z.L. Zhang, Y.B. Shi, and D.W. Pang, Fluorescent-magnetic-biotargeting multifunctional nanobioprobes for detecting and isolating multiple types of tumor cells, ACS Nano **5**(2), 761–770 (2011), https://doi.org/10.1021/nn1011336

[18] E.V. Groman, J.C. Bouchard, C.P. Reinhardt, and D.E. Vaccaro, Ultrasmall mixed ferrite colloids as multidimensional magnetic resonance imaging, cell labeling, and cell sorting agents, Bioconjugate Chem. **18**(6), 1763–1771 (2007), https://doi.org/10.1021/bc070024w

[19] M. Pilloni, J. Nicolas, V. Marsaud, K. Bouchemal, F. Frongia, A. Scano, G. Ennas, and C. Dubernet, PEGylation and preliminary biocompatibility evaluation of magnetite–silica nanocomposites obtained by high energy ball milling, Int. J. Pharmaceut. **401**, 103–112 (2010), https://doi.org/10.1016/j.ijpharm.2010.09.010

[20] R.Y. Hong, J.H. Li, J.M. Qu, J.J. Chen, and H.Z. Li, Preparation and characterization of magnetite/dextran nanocomposite as a precursor of magnetic fluid, Chem. Eng. J. **150**, 572–580 (2009), https://doi.org/10.1016/j.cej.2009.03.034

[21] I. Sharifi, H. Shokrollahi, and S. Amiri, Ferrite-based magnetic nanofluids used in hyperthermia applications, J. Magn. Magn. Mat. **324**(6), 903–915 (2012), https://doi.org/10.1016/j.jmmm.2011.10.017

[22] R. Hergt, S. Dutz, R. Muller, and M. Zeisberger, Magnetic particle hyperthermia: nanoparticle magnetism and materials development for cancer therapy, J. Phys. Condens. Matter **18**(38), S2919–S2934 (2006), https://doi.org/10.1088/0953-8984/18/38/S26

[23] V. Pašukonienė, A. Mlynska, S. Steponkienė, V. Poderys, M. Matulionytė, V. Karabanovas, U. Statkutė, R. Purvinienė, J.A. Kraśko, A. Jagminas, M. Kurtinaitienė, M. Strioga, and R. Rotomskis, Accumulation and biological effects of cobalt ferrite nanoparticles in human pancreatic and ovarian cancer cells, Medicina **50**, 237–244 (2014), https://doi.org/10.1016/j.medici.2014.09.009

[24] N. Sanpo, C.C. Berndt, C. Wen, and J. Wang. Transition metal-substituted cobalt ferrite nanoparticles for biomedical applications, Acta Biomater. **9**, 5830–5837 (2013), https://doi.org/10.1016/j.actbio.2012.10.037

[25] R. Žalneravičius, A. Paškevičius, M. Kurtinaitienė, and A. Jagminas, Size-dependent antimicrobial properties of the cobalt ferrite nanoparticles, J. Nanopart. Res. **18**, 300-1–10 (2016), https://doi.org/10.1007/s11051-016-3612-x

[26] V. Bėčytė, K. Mažeika, T. Rakickas, and V. Pakštas, Study of magnetic and structural properties of cobalt-manganese ferrite nanoparticles obtained by mechanochemical synthesis, Mat. Chem. Phys. **172**, 6–10 (2016), https://doi.org/10.1016/j.matchemphys.2015.11.029

[27] S. Solopan, A. Belous, A. Yelenich, L. Bubnovskaya, A. Kovelskaya, A. Podoltsev, I. Kondratenko, and S. Osinsky, Nanohyperthermia of malignant tumors. I. Lanthanum-strontium manganite magnetic fluid as potential inducer of tumor hyperthermia, Exp. Oncol. **33**, 130–135 (2011).

[28] M. Veverka, K. Zaveta, O. Kaman, P. Veverka, K. Knizek, E. Pollert, M. Burian, and P. Kaspar, Magnetic heating by silica-coated Co–Zn ferrite particles, J. Phys. D **47**(6), 065503 (2014), https://doi.org/10.1088/0022-3727/47/6/065503

[29] K. Mažeika, A. Mikalauskaitė, and A. Jagminas, Influence of interactions to the properties of ultrasmall $CoFe_2O_4$ nanoparticles estimated by Mössbauer study, J. Magn. Magn. Mater. **389**, 21–26 (2015), https://doi.org/10.1016/j.jmmm.2015.04.044

[30] S.J. Kim, S.W. Lee, and C.S. Kim, Mössbauer studies on exchange interactions in $CoFe_2O_4$, Jpn. J. Appl. Phys. **40**, 4897–4902 (2001), https://doi.org/10.1143/JJAP.40.4897

[31] B. Tian and G. Zerbi, Lattice-dynamics and vibrational spectra of polypyrrole, J. Chem. Phys. **92**(6), 3886–3891 (1990), https://doi.org/10.1063/1.457794

[32] S. Chikazumi, *Physics of Ferromagnetism* (Oxford University Press, New York, 2005) pp. 270–273.

[33] A. Pradeep, P. Priyadharsini, and G. Chandrasekaran, Structural, magnetic and electrical properties of nanocrystalline zinc ferrite, J. Alloy. Compd. **509**(9), 3917–3923 (2011), https://doi.org/10.1016/j.jallcom.2010.12.168

[34] V.M. Kalita, A.I. Tovstolytkin, S.M. Ryabchenko, O.V. Yelenich, S.O. Solopan, and A.G. Belous, Mechanisms of AC losses in magnetic fluids based on substituted manganites, Phys. Chem. Chem. Phys. **17**, 18087–18097 (2015), https://doi.org/10.1039/C5CP02822A

[35] S. Bedanta and W. Kleemann, Superparamagnetism, J. Phys. D **42**(1), 013001 (2008), https://doi.org/10.1088/0022-3727/42/1/013001

[36] S.A. Majetich and M. Sachan, Magnetostatic interactions in magnetic nanoparticle assemblies: energy, time and length scales, J. Phys. D **39**, R407–R422 (2006), https://doi.org/10.1088/0022-3727/39/21/R02

[37] C. Vázquez-Vázquez, M.A. López-Quintela, M.C. Buján-Núñez, and J. Rivas, Finite size and surface effects on the magnetic properties of cobalt ferrite nanoparticles, J. Nanopart. Res. **13**(4), 1663–1676 (2011), https://doi.org/10.1007/s11051-010-9920-7

[38] G. Herzer, Nanocrystalline soft magnetic materials, Phys. Scripta **49A**, 307–314 (1993), https://doi.org/10.1088/0031-8949/1993/T49A/054

[39] W.C. Nunes, L.M. Socolovsky, J.C. Denardin, F. Cebollada, A.L. Brandl, and M. Knobel, Role of magnetic interparticle coupling on the field dependence of the superparamagnetic relaxation time, Phys. Rev. B **72**, 212413-1–4 (2005), https://doi.org/10.1103/PhysRevB.72.212413

[40] J. Carrey, B. Mehdaoui, and M. Respaud, Simple models for dynamic hysteresis loop calculations of magnetic single-domain nanoparticles: Application to magnetic hyperthermia optimization, J. Appl. Phys. **109**(8), 083921 (2011), https://doi.org/10.1063/1.3551582

[41] B. Mehdaoui, A. Meffre, J. Carrey, S. Lachaize, L.M. Lacroix, M. Gougeon, B. Chaudret, and M. Respaud, Optimal size of nanoparticles for magnetic hyperthermia: A combined theoretical and experimental study, Adv. Funct. Mater., **21**(23), 4573–4581 (2011), https://doi.org/10.1002/adfm.201101243

$CoFe_2O_4$ IR $CoFe_2O_4$/POLIPIROLIO NANODALELIŲ MAGNETINIŲ SAVYBIŲ PALYGINIMAS

K. Mažeika [a], V. Bėčytė [a], Yu.O. Tykhonenko-Polishchuk [b], M.M. Kulyk [c], O.V. Yelenich [d], A.I. Tovstolytkin [b]

[a] *Fizinių ir technologijos mokslų centras, Vilnius, Lietuva*

[b] *NMA ir ŠMM Magnetizmo institutas, Kijevas, Ukraina*

[c] *ŠMM Fizikos institutas, Kijevas, Ukraina*

[d] *ŠMM Bendrosios ir neorganinės chemijos V.I. Vernadskio institutas, Kijevas, Ukraina*

Santrauka

$CoFe_2O_4$/polipirolio kompozitinės nanodalelės susintetintos pasitelkus planetarinį didelės energijos rutulinį malūną. Mesbauerio ir FTI spektroskopijos, magnetiniai matavimai ir peršviečianti elektroninė mikroskopija buvo panaudoti susintetintų medžiagų struktūrinėms ir magnetinėms savybėms nustatyti. Išsiskirianti specifinė nuostolių galia hipertermijai nustatyta veikiant nanodaleles 300 kHz dažnio ir 124 Oe amplitudės kintamu magnetiniu lauku. Lyginant $CoFe_2O_4$ ir $CoFe_2O_4$/polipirolio kompozitinių nanodalelių histerezės kilpas buvo pastebėti koercinės jėgos pokyčiai, paaiškinami dėl polipirolio įtakos pakitusia nanodalelių sąveika.